

A Study for Estimating Thermal Strain and Thermal Stress in Optical Fiber Coatings

by Yasuo Nakajima *, Hiroki Tanaka *, Kouji Mochizuki *, Kazuyuki Fuse *, Yoshihiro Arashitani *, Takuya Nishimoto *, Atsuyoshi Seno * and Mitsunori Okada *

ABSTRACT In general, optical fibers are coated with UV-curable resins--a soft primary coating and a hard secondary coating--to protect the glass. Under UV radiation curing heat is produced and it is known that, since the coefficient of thermal expansion (CTE) of the primary coating is greater than that of the secondary coating, a negative hydrostatic pressure is produced in the primary coating during the cooling process, resulting in a force acting to delaminate the primary coating from the glass^{1)~3)}. To achieve long-term reliability of optical fibers it is necessary to analyze the thermal strain and thermal stress that arise in the coatings of the fiber, and accordingly, in this work, we discuss methods for measuring the CTEs of the coatings and the modulus of elasticity of the secondary coating during the drawing process.

1. INTRODUCTION

Optical fibers are drawn with resin coatings that protect the glass. In general UV-curable resins are used for the coatings, and in most single-mode (SM) fibers a dual-coating structure is adopted. Each coating layer has an independent function in the protection of the glass. The coating in direct contact with the glass is known as the primary (P) coating, with the role of acting as a buffer against the external forces that can cause microbending. Accordingly the primary coating is designed to be soft, with a Young's modulus of 1 MPa or less, and in consideration of the conditions of use, the glass transition temperature T_g is lower than room temperature. The primary coating is then covered by a hard secondary (S) coating for protection against external forces, and generally speaking a material having a Young's modulus of 500 MPa or more and a T_g of 60°C or above is used.

During the drawing process the optical fiber is heated by an exothermic reaction as the UV-curable coating cures and by heat irradiated by the UV lamp, so that the temperature of the coatings rises above the T_g of the secondary coating. After UV lamp irradiation, the fiber is self-cooled to room temperature and then wound on a spool^{1)~4)}.

During the cooling process following curing, the secondary coating, since its T_g is higher than room temperature, transforms from the rubbery state to the glassy state. The primary coating, for its part, remains in the rubbery state as it cools to room temperature. The CTE of a polymer changes significantly at its T_g ¹⁾. This means that at

temperatures below the T_g of the secondary coating. The coefficient of thermal shrinkage of the primary coating is greater than that of the secondary coating. This CTE mismatch gives rise to strain at the primary/secondary interface, resulting in a force acting to delaminate the primary coating from the glass. Figure 1 is a schematic of CTE mismatch between the primary and secondary coatings, where β is cubic CTE, its subscript indicates the type of coating, and ΔT is the difference between the T_g of the secondary coating and room temperature.

Knowing the thermal strain of optical fiber coatings would be of great importance in terms of fiber reliability. The purpose of this study is to measure the CTEs of each of the coatings from the coatings of actual optical fibers, and further to determine the actual thermal strain produced in the coatings and further, the residual stress. Accordingly, for the measurement of CTE we used a thermo-mechanical analyzer (TMA) and to estimate residual

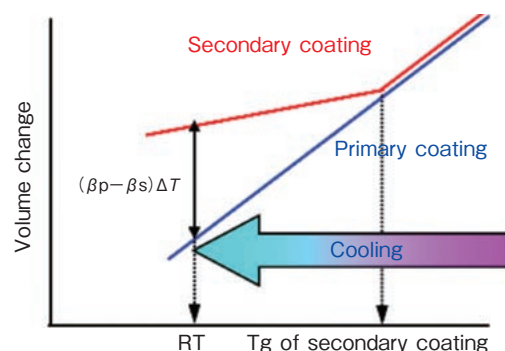


Figure 1 Schematic of CTE mismatch between primary and secondary coatings.

* FITEL-Photonics Lab., R&D Div.

stress we used a dynamic mechanical analyzer (DMA) to measure the modulus of elasticity of the secondary coating, modeling after the drawing process.

2. METHOD FOR MEASURING CTE OF OPTICAL FIBERS

2.1 Method for Preparing Samples

For the UV-curable resins used for the primary and secondary coatings, we used commercially available materials. The samples had outer diameters of 125/195/245 μm for the glass/primary coating/secondary coating respectively.

2.2 Preparing Samples for CTE Measurement

To measure the coefficients of thermal expansion of the optical fiber coatings, two types of coating samples were prepared. The first were standard dual-coated silica glass fiber samples, and the other were tube samples consisting of the coatings only.

The tube samples were prepared by pulling out the silica glass from the coated fiber in liquid nitrogen.

2.3 CTE Measurement by TMA

For CTE measurement we used a thermo-mechanical analyzer (TMA-40 from Mettler Toledo). The instrument was placed on a vibration isolation table and was cooled with liquid nitrogen to effect measurement from below room temperature,

Temperature conditions:

- cool from 25 to -100°C at a rate of $-10^{\circ}\text{C}/\text{min}$
- hold at -100°C for 10 min
- heat from -100 to 150°C at a rate of $10^{\circ}\text{C}/\text{min}$

In order not to apply load to the samples, CTE measurement was carried out at zero-load, and in two directions: longitudinal and radial. Since measurement at zero load is particularly sensitive to vibration, the vibration isolation table was essential.

CTE in the longitudinal direction of the fiber was measured in tensile mode. Samples with a measured length of 12.5 mm were held at both ends by copper wire and attached to the TMA instrument.

CTE in the radial direction of the fiber was measured in compression mode. The shape of the probe was a plane circle with a diameter of 3 mm, and the measured length was 245 μm , approximately the same as the outer diameter of the fiber.

3. METHOD FOR MEASURING RELAXATION MODULUS

3.1 Preparing Cured Film

In this work, we adopted the term relaxation modulus for the modulus of elasticity of the secondary coating that is determined modeling after the thermal history of the drawing process based on estimated residual stress.

In measuring the relaxation modulus, we used cured film. The UV-cured resins used for the secondary coating were

three commercially available materials having different values of T_g (A: high; B: middling; and C: low). The cured films were prepared by application to a glass substrate with a depth of 100 μm , and irradiation in nitrogen by a UV lamp (Fusion F450, D-bulb) with a UV dose of 1.0 J/cm^2 . Sample dimensions were 2(W) \times 20(L) \times 0.1(t) mm.

3.2 Relaxation Modulus Measurement by DMA

The relaxation modulus was measured by means of a DMS6100 made by SII Nano Technology with the cured film mounted on a tensile jig, using a time sweep of stress (at 1-sec intervals). In measuring, the film samples were mounted with chuck intervals of 20 mm, held at a temperature of 140°C for 40 min, and then, with strain applied to the sample, the temperature was lowered to 30°C at a rate of $1^{\circ}\text{C}/\text{min}$, and strain was applied until finally the strain on the sample reached 2%. Then, they were held at a strain of 2% for 300 min. When the stress obtained was divided by the cross-sectional area of the film, it was possible to determine the secondary coating modulus, modeling after the drawing process. Figure 2 shows the temperature-strain profile.

Using the same instrument and with a temperature sweep at a frequency of 1 rad/sec, the storage modulus of elasticity (E'), loss modulus of elasticity (E'') and $\tan \delta$ were measured in the range of $50\sim 150^{\circ}\text{C}$. In this work the glass transition temperature T_g was taken as the peak value of $\tan \delta$ ¹⁾.

3.3 Measuring Young's Modulus

Young's modulus was measured using a Tensilon-type tensile tester (RTC1310A from A&D). With film samples measuring 6(W) \times 50(L) \times 0.03(t) mm, chuck intervals of 25 mm, pulled at room temperature with a strain rate of 1 mm/min, the Young's modulus was determined from 2.5% strain. Table 1 shows the results for Young's modulus and T_g .

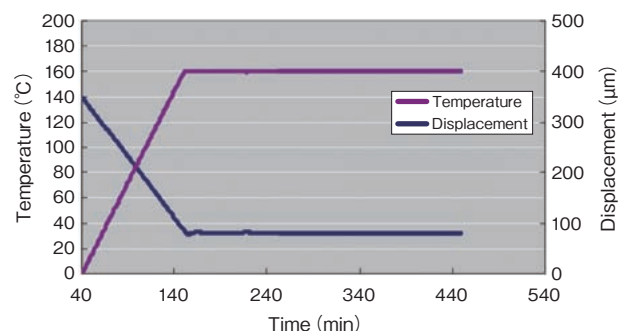


Figure 2 Conditions of measurement.

Table 1 Properties of secondary coatings.

	Young's Modulus	Glass Transition Temp.
A	690 MPa	110°C
B	760 MPa	84°C
C	453 MPa	63°C

4. RESULTS AND DISCUSSION

4.1 CTE Measurement by Tensile Mode

Figure 3 shows the results of CTE measurements by tensile mode. As can be seen, thermal shrinkage of the fiber samples with glass is remarkably lower than that of the tube samples consisting of coating resins only.

The linear CTE of silica glass is a mere $0.5 \times 10^{-6} \text{ K}^{-1}$, and since the primary coating adheres to the silica glass fiber, it can readily be seen that the longitudinal thermal expansion of the secondary coating will be restricted by the silica glass.

The CTE of the samples was calculated for two separate temperature ranges. Since the CTE of a polymer changes significantly at the T_g , we made the separation at -50°C , the T_g of the primary coating. Table 2 shows the results of CTE measurement by tensile mode.

4.2 CTE Measurement by Compression Mode

Figure 4 shows the results of CTE measurement by compression mode. As can be seen, radial thermal shrinkage of the fiber samples is greater than that of the tube samples.

The CTEs of the fiber samples and tube samples were calculated for the same temperature ranges as in the tensile mode tests. Table 3 shows the results for CTE measured by compression mode.

4.3 Estimation of CTE for Each Coating

The cubic CTEs of the primary coating and secondary coating were estimated from the tensile-mode and compression-mode measurements of CTE for the fiber samples and the tube samples. The method of estimating cubic CTE for each coating was as follows:

At temperatures ranging from 25°C to -50°C , in the case of the tube samples the primary coating is in the rubbery state and the Young's modulus is significantly smaller

than that of the secondary coating, so that the secondary coating can expand and contract freely. Since the cubic CTE of the secondary coating is two times the linear CTE in the radial direction plus the linear CTE in the longitudinal direction, we may determine the cubic CTE of the secondary coating from

$$\beta_S = \alpha_{SL} + 2 \times \alpha_{SR} \quad (1)$$

where: β_S is the cubic CTE of the secondary coating
 α_{SL} is the linear CTE of the secondary coating in the longitudinal direction
 α_{SR} is the linear CTE of the secondary coating in the radial direction

With respect to the fiber samples, the primary coating adheres to the silica glass, so that the secondary coating cannot expand and contract freely and the thermal expansion of the coatings is restrained by the silica glass fiber. Since the CTE of silica glass is remarkably lower than that of the coatings, thermal expansion can be neglected. Accordingly we may determine the cubic CTE of the primary coating from

$$D_G + (D_P - D_G) \times \left(1 + \frac{\beta_P}{2}\right) + (D_S - D_P) \times \left(1 + \frac{\beta_P}{2}\right) = D_S \times (1 + \alpha_{FR}) \quad (2)$$

where: β_P is the cubic CTE of the primary coating
 β_S is the cubic CTE of the secondary coating
 α_{FR} is the linear CTE of the primary coating in the radial direction
 D_G is the outer diameter of the silica glass ($125 \mu\text{m}$)
 D_P is the outer diameter of the primary coating ($195 \mu\text{m}$)
 D_S is the outer diameter of the secondary coating ($245 \mu\text{m}$)

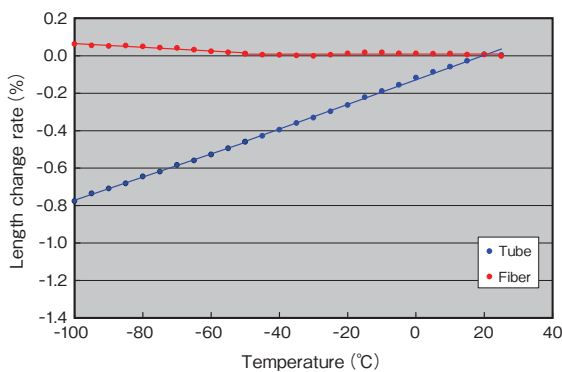


Figure 3 CTE measurement by tensile mode.

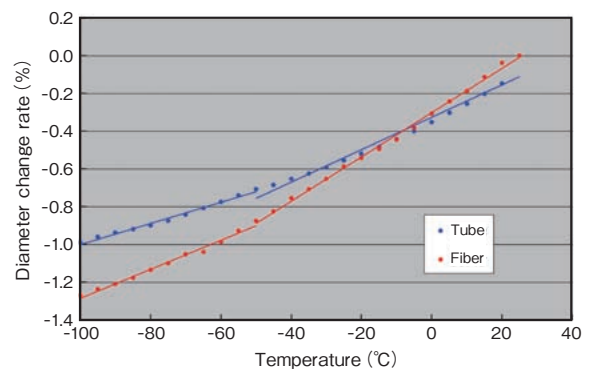


Figure 4 CTE measurement by compression mode.

Table 2 Longitudinal CTE measurement by tensile mode.

Sample	Linear coefficient of thermal expansion	
	25 to -50°C	-50 to -100°C
Fiber	$0.004 \times 10^{-4} \text{ K}^{-1}$	$-0.10 \times 10^{-4} \text{ K}^{-1}$
Tube	$0.66 \times 10^{-4} \text{ K}^{-1}$	$0.62 \times 10^{-4} \text{ K}^{-1}$

Table 3 Radial CTE measurement by compression mode.

Sample	Linear coefficient of thermal expansion	
	25 to -50°C	-50 to -100°C
Fiber	$1.17 \times 10^{-4} \text{ K}^{-1}$	$0.77 \times 10^{-4} \text{ K}^{-1}$
Tube	$0.86 \times 10^{-4} \text{ K}^{-1}$	$0.56 \times 10^{-4} \text{ K}^{-1}$

Table 4 shows the estimated values of cubic CTE for each coating. One-third of the cubic CTE is the linear CTE. At temperatures between -50°C and 25°C , that is to say where the primary coating is rubbery and the secondary coating is glassy, the CTE of the primary coating was 2.7 times higher than that of the secondary coating. Further the CTE of the primary coating in the rubbery state was 1.8 times higher than in the glassy state. It was estimated that this would be approximately 3 times, but further confirmation is required for the fact that it was lower than predicted at temperatures below -50°C . In this estimation, since the secondary coating is always glassy at room temperature, we calculated the CTE of the primary coating taking the secondary coating CTE as $2.38 \times 10^{-4} \text{ K}^{-1}$.

4.4 Internal Strain in Fiber Coating

Next we investigated internal thermal strain in the secondary coating by means of measurement of CTE. Figure 5 shows results for thermal expansion of tube samples by tensile mode in the $-100 \sim 150^{\circ}\text{C}$ temperature range. In the area inside the dotted circle in Figure 5, thermal shrinkage of the tube samples occurred at approximately 90°C , a temperature that is close to the T_g of the secondary coating.

4.5 Verification of Internal Strain in Fiber Coatings

We verified that the thermal shrinkage observed in Figure 5 is due to internal strain in the secondary coating by means of the method described below.

In this method, tube samples were aged under zero load conditions using the following program:

Table 4 Estimated cubic CTE for each coating.

Sample	Cubic coefficient of thermal expansion	
	25 to -50°C	-50 to -100°C
Primary	$6.34 \times 10^{-4} \text{ K}^{-1}$	$3.54 \times 10^{-4} \text{ K}^{-1}$
Secondary	$2.38 \times 10^{-4} \text{ K}^{-1}$	$2.38 \times 10^{-4} \text{ K}^{-1}$

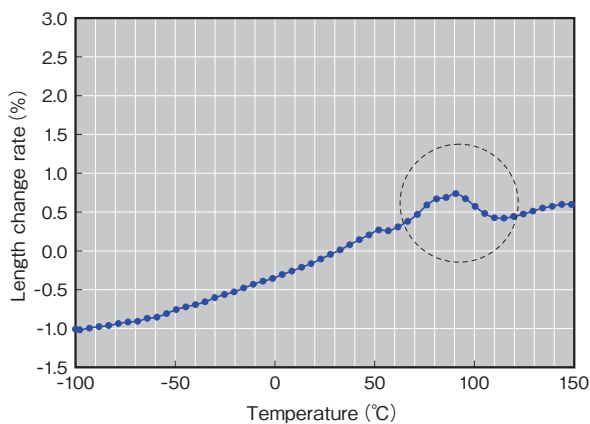


Figure 5 Thermal expansion of tube sample by tensile mode.

Temperature conditions:
 heat from 25 to 150°C at a rate of $10^{\circ}\text{C}/\text{min}$
 cool from 150 to 25°C at a rate of $10^{\circ}\text{C}/\text{min}$

The linear thermal expansion of tube samples subjected to the above thermal profile was then measured under the same conditions as in Section 4.4 above.

Figure 6 shows the results for the CTE of aged tube samples. In contrast to the thermal shrinkage observed around 90°C in Figure 5, no thermal shrinkage was observed in the aged tube samples. Thermal shrinkage was evidently eliminated through zero-load aging.

These results suggest that the secondary coating has latent internal strain, and that internal strain is caused by the curing process at the time of drawing. From the fact that internal strain gives rise to longitudinal shrinkage, it is suggested that the strain that has been extended in the longitudinal direction accumulates in the secondary coating.

4.6 Relaxation Modulus in the Secondary Coating

Figure 7 shows results measured by the method described in Section 3 above. For any of the resins examined, the modulus of elasticity increased with cooling from 140°C to 30°C , and the slopes of the initial rises are substantially the same, though the maximum values differ.

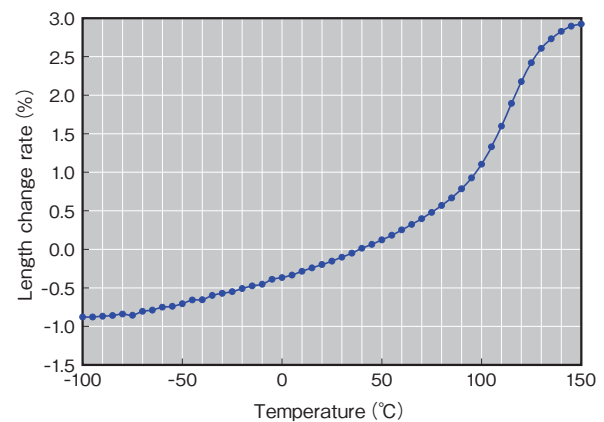


Figure 6 Thermal expansion of aged tube samples by tensile mode.

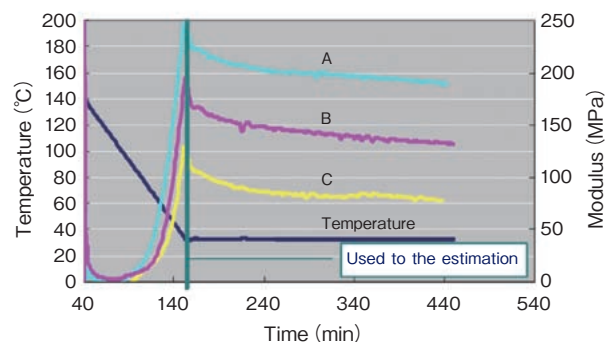


Figure 7 Results for relaxation modulus.

Secondary coating A was the highest and secondary coating C the lowest. When subsequently held at 30°C under an applied strain of 2%, the modulus of elasticity decreased gradually over time. Even at the end of the measured time, the modulus of elasticity still continued to decrease, but it is presumed that it is approaching a substantially equilibrium condition.

The moduli shown in Figure 7 suggest that there is a correlation with the T_g of the secondary coatings shown in Table 1. Secondary coating T_g increases in sequence for coatings A, B and C. This order is the same as that of the moduli shown in Figure 7. On the other hand, it also suggests that there is no correlation between the Young's modulus of the cured films and the moduli in Figure 7.

Generally speaking, resins that are rubbery at temperatures above T_g are easily relaxed. The difference between pre-aging temperature of 140°C and secondary coating T_g is 30°C for material A, 53°C for material B and 77°C for material C, so that the temperature range for relaxation is broader for resins with lower T_g . The results obtained here corroborate this expectation, demonstrating that the degree of relaxation is quantitative.

The samples are being cooled from a temperature above T_g to room temperature under constant applied strain, and this process models after the drawing of actual fibers. In the actual drawing process, the glass surface is covered with UV-curable resin coatings, which are then irradiated under a UV lamp and heated by the exothermic curing reaction and by the radiant heat. The optical fiber is then cooled to room temperature and wound on a spool. In this condition the adhesiveness of the primary coating binds it to the glass. For this reason the coating is cooled under conditions of constant strain.

The method used in this work does not, strictly speaking, reproduce the actual drawing process, but it holds forth the promise of enabling a quantitative analysis based on evaluation of residual stress in the optical fiber coatings. Specifically, the measured values obtained by this method have been effective in analyzing the stresses caused by the coatings at the glass/primary interface ^{1), 2)}.

5. CONCLUSIONS

5.1 Determining CTE for Each Coating

By conducting measurements on fiber samples with silica glass and on tube samples, from both the longitudinal direction and the radial direction, we were able to determine the cubic CTE of each coating. It was confirmed that a method using a thermal mechanical analyzer (TMA) was an effective means for measuring the CTE of optical fiber coatings.

According to Reference 1) the CTE of the primary is approximately 3 times higher than that of the secondary. (The original document is Reference 5)). In the method described in this work we were able to determine the accurate CTEs necessary to the calculation of accurate

thermally induced residual stresses in dual-coated optical fibers.

5.2 Internal Strain in Optical Fiber Coatings

It became clear that the secondary coating had internal strain. The fact that thermal shrinkage of tube samples occurs at approximately 90°C, corresponding to the T_g of the secondary material, means that this internal strain can be released at temperatures above the T_g of the secondary coating.

It was also confirmed that for tube samples, thermal contraction in the longitudinal direction disappears when the secondary coating is aged under zero load at temperatures above T_g .

As described above, the internal strain in the secondary coating is formed in the curing process during optical fiber drawing. It is assumed that this is caused by the secondary coating being cured at temperatures above T_g , internal stress in the secondary coating being caused by the mismatch in CTE between the primary coating and secondary coating during the cooling process.

5.3 Relaxation Modulus of the Secondary Coating

The modulus of a secondary coating that is determined modeling after the thermal history of the drawing process, based on estimated residual stress, is termed the relaxation modulus. The measuring method involves aging the secondary coating above the T_g while strain is applied and finding the stress when cooled to room temperature. It became clear that the correlation of the relaxation modulus to T_g was high.

This method has not yet been able strictly speaking to reproduce the actual drawing process, but since it makes possible a quantitative analysis based on evaluating residual stress in the optical fiber coatings, it is expected to prove useful in analyzing the stress produced by the coatings at the glass/primary interface.

REFERENCES

- 1) C. J. Aloisio, W. W. King, R. C. Moore: A viscoelastic analysis of thermally induced residual stresses in dual coated optical fibers, Proc. 44th IWCS, p. 139 (1995).
- 2) W. W. King, C. J. Aloisio: Thermomechanical Mechanism for Delamination of Polymer Coatings From Optical Fibers, Journal of Electronic Packaging, 119, p. 133 (1997).
- 3) Win-Jin Chang: Viscoelastic analysis of hydrostatic pressure induced optical effects in double-coated optical fibers, J. Appl. Phys., Vol. 93, No. 1, 1 January (2003).
- 4) Y. Arashitani, Y. Nakajima, Y. Gamoh, H. Tanaka, M. Okada: A Method for Estimating the Contribution of Modulus and T_g on the Residual Stress in Optical Fiber Coatings, Proc. 53rd IWCS, p. 285 (2004).
- 5) J. D. Ferry: Viscoelastic Properties of Polymers, John Wiley & Sons (1980).